J Fusion Energ (2010) 29:353–359
DOI 10.1007/s10894-010-9287-x

ORIGINAL RESEARCH

# Neutron Emission Spectra of Some Structural Fusion Materials at 26.8 and 45.2 MeV Alpha Incident Energies

**A. Kaplan · A. Aydin · E. Tel · H. Büyükuslu**

Published online: 23 March 2010
© Springer Science+Business Media, LLC 2010

**Abstract** In this study, neutron-emission spectra produced by ($\alpha$,*xn*) reactions for some structural fusion materials such as $^{27}$Al, $^{53}$Cr, $^{56}$Fe and $^{58,60,62}$Ni have been investigated. Hybrid model, geometry dependent hybrid model and full exciton model have been used to calculate the pre-equilibrium neutron-emission spectra. For the reaction equilibrium component, Weisskopf–Ewing model calculations have been preferred. The mean free path parameter's effect for ($\alpha$,*xn*) neutron-emission spectra has been examined. The obtained results have been discussed and compared with the available experimental data and found agreement with each other.

**Keywords** Alpha-induced reactions · Geometry dependent hybrid model · Neutron emission spectra · ($\alpha$,*xn*) Cross-section

## Introduction

Along with the ongoing efforts to utilize fusion as an energy source, there is renewed interest in fusion neutron source applications for purpose such as resource utilization and long-lived radioactive waste transmutation with fusion–fission hybrid systems [1–4]. New material technologies are needed to meet development of innovative fuel cycle and hybrid reactor technologies [5–11]. A special emphasis is being given for the development of the structural materials because the success of the fusion reactors is largely dependent on the development of these materials. The development of adequate structural materials is a major step towards fusion reactors becoming an efficient source of energy, particularly if the promise of an environmentally safe machine is to be realized. These materials can be classified their activation characteristics. C, Si, Ti, Fe, Cr and V are considered as low activation elements while elements such as Al, Ni, Ag, Co, Nb are some of the high activation materials [12, 13]. The choice of structural materials for combined first-wall-breeding-blanket components depends not only on mechanical properties, compatibility with other materials and irradiation performance, but also on their radiological properties [14].

Because materials are required in the vicinity of the plasma to interact with fusion neutrons to extract either nuclear energy for conversion into electricity, or charged particle ashes to maintain plasma operation, radioactivity is induced in these first wait and blanket materials when they are interacting with neutrons. However, by carefully selecting the first wall and blanket materials, a fusion power plant may minimize or eliminate the induced radioactivity [15]. Eighty per cent of the energy released by the DT fusion reaction is transferred by 14 MeV neutrons to the first wall and the breeding blanket. The remaining 20% is carried by $\alpha$ particles arising from the same reaction, which, together with other low energy neutral and charged particles, will induce sputtering, erosion and blistering in plasma facing materials [13, 16].

A. Kaplan (✉) · H. Büyükuslu
Faculty of Arts and Sciences, Department of Physics, Süleyman Demirel University, Isparta, Turkey
e-mail: kaplan@fef.sdu.edu.tr

A. Aydin
Faculty of Arts and Sciences, Department of Physics, Kırıkkale University, Kirikkale, Turkey

E. Tel
Faculty of Arts and Sciences, Department of Physics, Gazi University, Ankara, Turkey

Since the experimental data of charged particle induced reactions are scarce and there are significant discrepancies among experimental data of different laboratories, the self-consistent calculation and analysis using nuclear theoretical models are very important and interesting [17]. Especially, Integral data on cross-sections of alpha induced reaction on iron are important for many reasons. Systematic study of production cross-sections and isomeric ratios is useful for investigation of nuclear structure and of the basic mechanisms of nuclear reactions [18–20]. In a fusion reactor design, neutron reaction cross-section data are required and the evaluated values in nuclear data files are usually used for the neutronics calculation. It is therefore very important to carry out benchmark experiments with candidate materials for a fusion reactor and to discuss their results in order to validate the evaluated nuclear data [21]. Therefore, new nuclear cross-section data are needed to improve the theoretical predictions of neutron and charged particle production, shielding requirements, activation, radiation heating, and material damage [22]. Additionally, data obtained from various techniques are necessary to develop additional nuclear theoretical calculation models to explain nuclear reaction mechanisms and the properties of the excited states for different energy ranges [23]. The observation of a forward peaked hard component in the continuous spectra of light ejectiles and the high energy tails seen in the excitation functions of activation cross-sections induced by α-particles, contains important information about the reaction mechanism. Several models [24–29] have been proposed to explain the emission of energetic light particles by the equilibration process (pre-equilibrium emission) from the nuclear system excited at medium energies. Predictions from these models as to excitation functions and the energy spectra of the emitted particles compared well with the existing experimental data [30].

In this study, neutron emission spectra for some structural fusion materials such as $^{27}$Al, $^{53}$Cr, $^{56}$Fe and $^{58,60,62}$Ni have been investigated for an incident alpha energy at 26.8, and 45.2 MeV. The neutron emission spectra for (α,*xn*), reactions have been calculated by equilibrium and pre-equilibrium reaction mechanisms. Also, the mean free path parameter's effect for (α,*xn*) neutron-emission spectra has been examined. The pre-equilibrium results have been calculated by using the hybrid model, the geometry dependent hybrid (GDH) model and full exciton model. The reaction equilibrium component has been calculated with a traditional compound nucleus model developed by Weisskopf–Ewing (WE). Calculation results have been also compared with the available measurements in literature.

## Calculation Methods

### Full Exciton Model

The calculations of the full exciton model with PCROSS code taking into account the direct gamma emission use the initial exciton number as $n_o = 1$. Equilibrium exciton number is taken equal to $\sqrt{1.4gE}$, as was suggested in Ref. [31], after Pauli correction is modified. Single particle level density parameter, $g$, was equal to $A/13$ in the full exciton model calculation, where $A$ is the mass number. Level density expression given by Dilg et al. [32] was used in the evaporation model calculation. Particle–hole state density expression reported by Williams [33] was used in the pre-equilibrium model calculation. The reaction cross-sections and the inverse cross-sections were obtained using the optical potential parameters by Wilmore and Hodgson [34], Becchetti and Greenless [35], Huizenga and Igo [36] for neutrons, protons and alpha particles, respectively. The compound nucleus reactions occur on a very much longer time scale ($\cong 10^{-16}$–$10^{-18}$ s). This process can be described adequately by the Weisskopf–Ewing. Compound nucleus wave function is very complicated, involving a large number of particle–hole excitations to which statistical considerations are applicable. In this theory, the spectra of the emitted particles are approximately Maxwellian, and the angular distributions of emitted particles are symmetric about 90 degrees.

### Equilibrium Model

Equilibrium emission is calculated according to Weisskopf–Ewing (WE) model [37] by neglecting angular momentum. In the evaporation, the basic parameters are binding energies, inverse reaction cross-section, the pairing, and the level-density parameters. The reaction cross-section for the incident channel $a$ and exit channel $b$ can be written as

$$\sigma_{ab}^{\mathrm{WE}} = \sigma_{ab}(E_{\mathrm{inc}})\frac{\Gamma_b}{\sum_{b'}\Gamma_{b'}} \tag{1}$$

where $E_{\mathrm{inc}}$ is the incident energy. In (1), $\Gamma_b$ can be also expressed as

$$\Gamma_b = \frac{2s_b+1}{\pi^2\hbar^2}\mu_b\int \mathrm{d}\varepsilon\sigma_b^{inv}(\varepsilon)\varepsilon\frac{\omega_1(U)}{\omega_1(E)} \tag{2}$$

where $U$, $\mu_b$, $s_b$ are the excitation energy of the residual nucleus, the reduced mass and the spin, respectively. The total single-particle level density is taken as,

$$\omega_1(E) = \frac{1}{\sqrt{48}}\frac{\exp\left[2\sqrt{\alpha(E-D)}\right]}{E-D}; \qquad \alpha = \frac{6}{\pi^2}g \tag{3}$$

where $\sigma_b^{\text{inv}}$, $E$, $D$ and $g$ are the inverse reaction cross-section, the excitation energy of the compound nucleus, the pairing energy and the single particle level density, respectively.

## Pre-Compound Hybrid and Geometry Dependent Hybrid Model Calculations

Pre-equilibrium processes play an important role in nuclear reactions induced by light projectiles with incident energies above about 8–10 MeV. Starting with the introduction of pre-equilibrium reactions, a series of semi classical models of varying complexities have been developed for calculating and evaluating particle emissions in the continuum. A first model to treat intermediate process is the intranuclear cascade model (INC), where classical nucleon trajectories are followed, assuming that nucleons collide pairwise with rate and angular distributions given by the measured free nucleon–nucleon scattering results [38]. The hybrid model for pre-compound decay is given by Blann and Vonach [39] as

$$\frac{\mathrm{d}\sigma_\upsilon(\varepsilon)}{\mathrm{d}\varepsilon} = \sigma_R P_\upsilon(\varepsilon)$$

$$P_\upsilon(\varepsilon)\mathrm{d}\varepsilon = \sum_{\substack{n=n_0 \\ \Delta n=+2}}^{\bar{n}} [{}_n\chi_\upsilon N_n(\varepsilon,U)/N_n(E)]g\,\mathrm{d}\varepsilon[\lambda_c(\varepsilon)/(\lambda_c(\varepsilon) \tag{4}$$

where $\sigma_R$ is the reaction cross section, ${}_n\chi_\upsilon$ is the number of particle type $\upsilon$ (proton or neutron) in $n$ exciton hierarchy, $P_\upsilon(\varepsilon)\mathrm{d}\varepsilon$ represents number of particles of the $\upsilon$ (neutron or proton) emitted into the unbound continuum with channel energy between $\varepsilon$ and $\varepsilon + \mathrm{d}\varepsilon$. The quantity in the first set of square brackets of (4) represents the number of particles to be found (per MeV) at a given energy $\varepsilon$ for all scattering processes leading to an "$n$" exciton configuration. $\lambda_c(\varepsilon)$ is emission rate of a particle into the continuum with channel energy $\varepsilon$ and $\lambda_+(\varepsilon)$ is the intranuclear transition rate of a particle. It has been demonstrated that the nucleon–nucleon scattering energy partition function $N_n(E)$ is identical to the exciton state density $\rho_n(E)$, and may be derived by the certain conditions on N–N (nucleon–nucleon) scattering cross sections [39]. The second set of square brackets in (4) represents the fraction of the $\upsilon$ type particles at an energy which should undergo emission into the continuum, rather than making an intranuclear transition. The $D_n$ represents the average fraction of the initial population surviving to the exciton number being treated.

The INC calculations results indicated that the exciton model gave only a prescription for calculating the shape of the pre-equilibrium spectrum and the exciton model deficiency resulted from a failure to properly reproduce enhanced emission from the nuclear surface [29, 40, 41]. In order to provide a first order correction for this deficiency the hybrid model was reformulated by Blann [24, 25, 42, 43]. This model, known as geometry dependent hybrid model (GDH) has been developed considered as density distribution of nuclei by Blann and Vonach [39].

In the density dependent version, the GDH takes into account the density distribution of the nucleus [39, 43]. This means a longer mean free path at the surface of the nucleus because of a lower density, and a limit to the depth of the holes below the Fermi energy. The differential emission spectrum is given in the GDH as

$$\frac{\mathrm{d}\sigma_\upsilon(\varepsilon)}{\mathrm{d}\varepsilon} = \pi\hat{\lambda}^2 \sum_{\ell=0}^{\infty} (2\ell+1)T_\ell P_\upsilon(\ell,\varepsilon) \tag{5}$$

where $\hat{\lambda}$ is the reduced de Broglie wavelength of the projectile and $T_\ell$ represents the transmission coefficient for the $l$th partial wave. $P_\upsilon(\ell,\varepsilon)$ is number of particles of the type $\upsilon$ (neutrons and protons) emitted into the unbound continuum with channel energy between $\varepsilon$ and $\varepsilon + \mathrm{d}\varepsilon$ for the $\ell$th partial wave. The GDH model is made according to incoming orbital angular momentum $\ell$ in order to account for the effects of the nuclear-density distribution. This leads to increased emission from the surface region of the nucleus, and thus to increased emission of high-energetic particles. In this way the diffuse surface properties sampled by the higher impact parameters were crudely incorporated into the pre-compound decay formalism in the GDH.

There is a strong dependence of the calculated emission spectra on the parameter of matrix element $K$ if the parameterizations proposed by Cline [44, 45] are used in the calculations of internal transitions rates $\lambda^i(i = +,-)$. In order to avoid such a strong dependence, using the parameterization of transition rate proposed by Blann [46] is preferred by considering experimental data and approximation based on Pauli principle. Using this parameterization and considering the particle–hole state densities from the formula by Williams [33] one can obtain the expressions found by Machner [47] for internal transition rates:

$$\lambda^+(E,n) = \frac{1}{k_{\text{mfp}}}\left(1.4\times10^{21}E' - \frac{2}{n+1}6\times10^{18}E'^2\right) \tag{6}$$

$$\lambda^-(E,n) = \frac{1}{k_{\text{mfp}}}\frac{(n-1)(n-2)ph}{(gE')^2} \times \left(1.4\times10^{21}E' - \frac{2}{n-1}6\times10^{18}E'^2\right)$$

Blann's parameterization for internal transition rate calculation involves the introduction of the mean free path parameter, $k_{\text{mfp}}$. This parameter allows an increase in mean free path, with simulation of effect, which is not considered in the calculations, such as conservation of parity and angular momentum in intra-nuclear transitions.

## Result and Discussion

In the calculations of the hybrid and GDH model, the code as ALICE/ASH was used. The ALICE/ASH code is an advanced and modified version of the ALICE codes [48]. The generalized superfluid [49] has been applied for nuclear level density calculations in the ALICE/ASH code. The ALICE-91 [50] and ALICE/ASH codes use the initial exciton number as $n_o = 3$. But in these models the different neutron ($n$) and proton ($p$) exciton numbers are used in the pre-equilibrium GDH model calculations. The mean free path parameter, $k_{\mathrm{mfp}}$, in ALICE/ASH code is controlled by the COST value which is the multiplication factor for nucleon free path. The mean free paths are multiplied by COST +1 in cross-section calculations. In details, the other code model parameters can be found in Ref. [48]. The calculations of the full exciton model with PCROSS code [51] taking into account the direct gamma emission use the initial exciton number as $n_o = 1$. The formulas and parameters used for the PCROSS code can be seen in detail Ref. [52].

In this study, the neutron-emission spectra produced by ($\alpha$,$xn$) reactions for some for some structural fusion materials such as $^{27}$Al, $^{53}$Cr, $^{56}$Fe and $^{58,60,62}$Ni have been calculated with the equilibrium and pre-equilibrium reaction models in Figs. 1, 2, 3, 4, 5, 6, 7, 8, 9, 10, and 11. It is clear that the compound process dominates at the low neutron emission energy up to 10 MeV. Generally for all reactions, the calculated neutron emission spectra by using ALICE/ASH for the equilibrium with Weisskopf–Ewing model calculations are in agreement with the experimental data at low energy region up to 8–12 MeV except the $^{27}$Al($\alpha$,$xn$) reaction calculations in Fig. 1. $^{27}$Al($\alpha$,$xn$) reaction equilibrium calculations in good agreement up to 20 MeV. Above 10 MeV, the Weisskopf–Ewing model can not calculate emission spectra (even if all the calculation parameters are changed). The equilibrium calculations with Weisskopf–Ewing model don't include angular momentum effects. In this theory, compound nucleus wave function is very complicated, involving a large number of particle-hole excitations to which statistical considerations are applicable, the spectra of the emitted particles are approximately Maxwellian, and the angular distributions of emitted particles are symmetric about 90 degrees.

The pre-equilibrium model calculations are in good agreement with the experimental data except the $^{27}$Al($\alpha$,$xn$) reaction (Fig. 1) in this study. Pre-Equilibrium calculations are upper the experimental data in Fig. 1 along the emission energy. Generally, the calculated emission spectra with hybrid model are below the GDH model and close the experimental data. $^{60}$Ni($\alpha$,$xn$) and $^{62}$Ni($\alpha$,$xn$) pre-equilibrium calculations are best agreement with the experimental data at the 26.8 MeV $\alpha$ particle energy. The reason is that

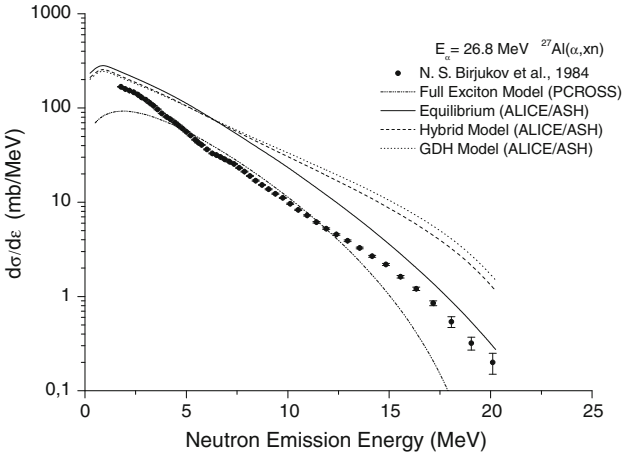


**Fig. 1** The comparison of neutron emission spectra of $^{27}$Al($\alpha$,$xn$) reaction with the values reported in literature at 26.8 MeV incident neutron energy. Experimental values were taken from Ref. [53]

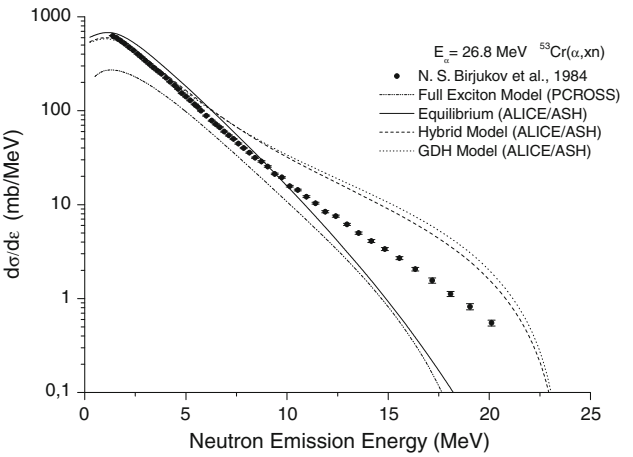


**Fig. 2** The comparison of neutron emission spectra of $^{53}$Cr($\alpha$,$xn$) reaction with the values reported in literature at 26.8 MeV incident neutron energy. Experimental values were taken from Ref. [53]

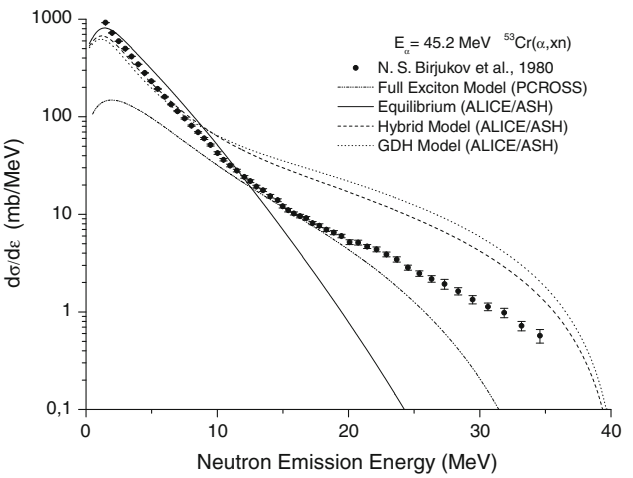


**Fig. 3** The comparison of neutron emission spectra of $^{53}$Cr($\alpha$,$xn$) reaction with the values reported in literature at 45.2 MeV incident neutron energy. Experimental values were taken from Ref. [53]

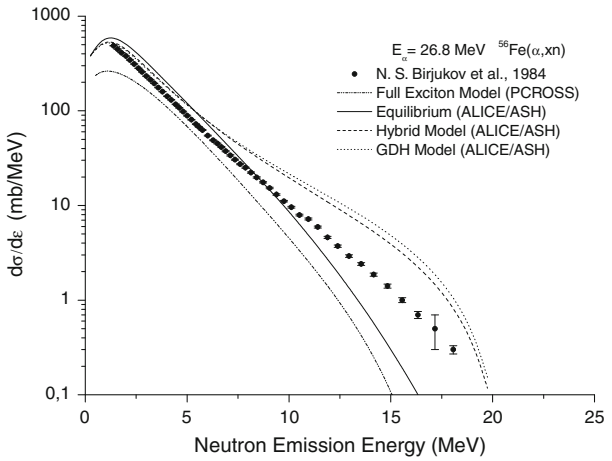


**Fig. 4** The comparison of neutron emission spectra of $^{56}$Fe(α,*xn*) reaction with the values reported in literature at 26.8 MeV incident neutron energy. Experimental values were taken from Ref. [53]

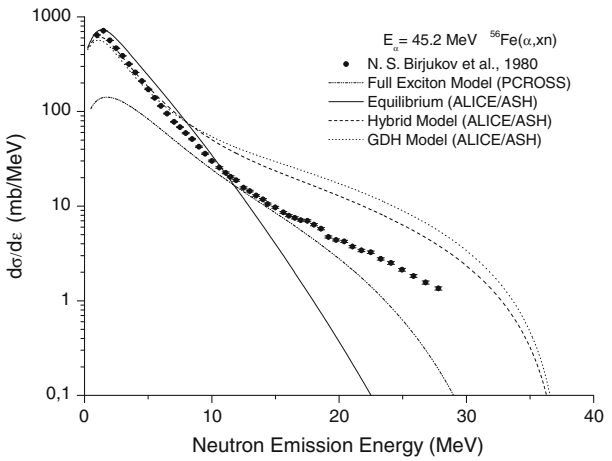


**Fig. 5** The comparison of neutron emission spectra of $^{56}$Fe(α,*xn*) reaction with the values reported in literature at 45.2 MeV incident neutron energy. Experimental values were taken from Ref. [53]

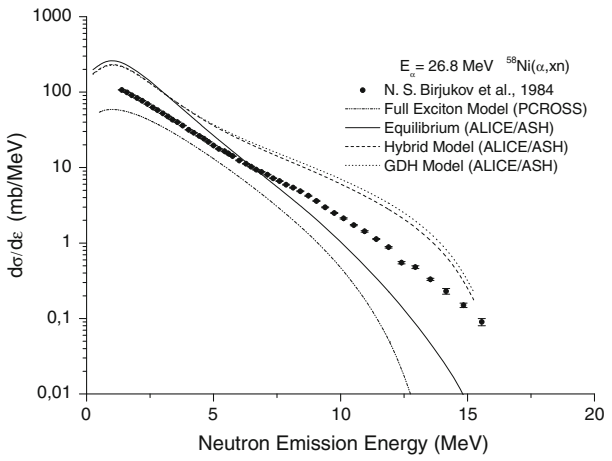


**Fig. 6** The comparison of neutron emission spectra of $^{58}$Ni(α,*xn*) reaction with the values reported in literature at 26.8 MeV incident neutron energy. Experimental values were taken from Ref. [53]

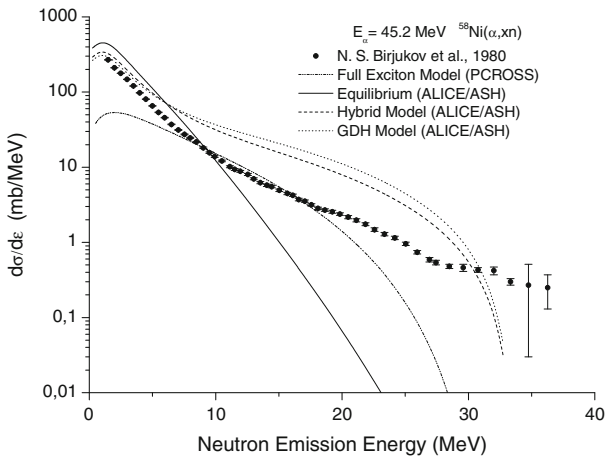


**Fig. 7** The comparison of neutron emission spectra of $^{58}$Ni(α,*xn*) reaction with the values reported in literature at 45.2 MeV incident neutron energy. Experimental values were taken from Ref. [53]

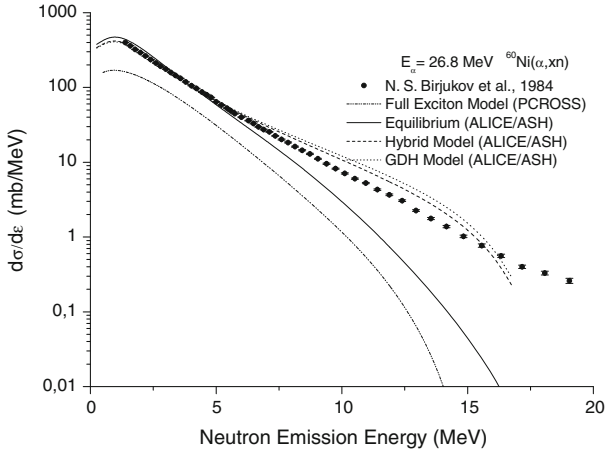


**Fig. 8** The comparison of neutron emission spectra of $^{60}$Ni(α,*xn*) reaction with the values reported in literature at 26.8 MeV incident neutron energy. Experimental values were taken from Ref. [53]

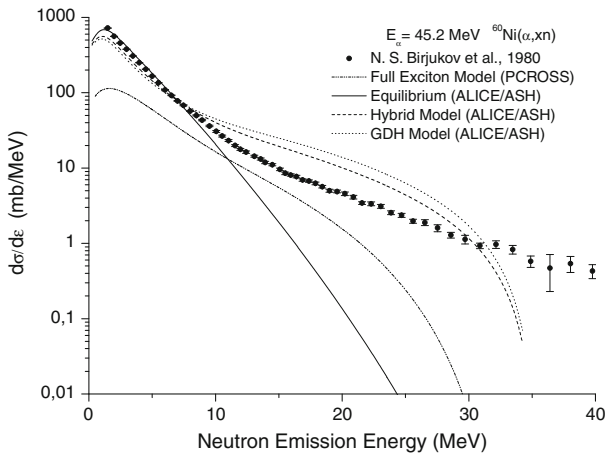


**Fig. 9** The comparison of neutron emission spectra of $^{60}$Ni(α,*xn*) reaction with the values reported in literature at 45.2 MeV incident neutron energy. Experimental values were taken from Ref. [53]

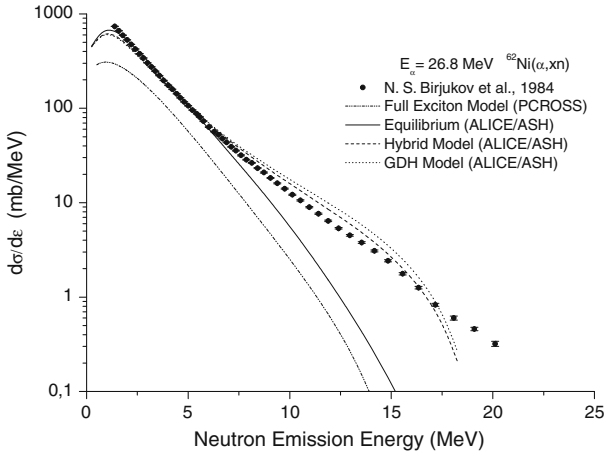


**Fig. 10** The comparison of neutron emission spectra of $^{62}$Ni(α,*xn*) reaction with the values reported in literature at 26.8 MeV incident neutron energy. Experimental values were taken from Ref. [53]

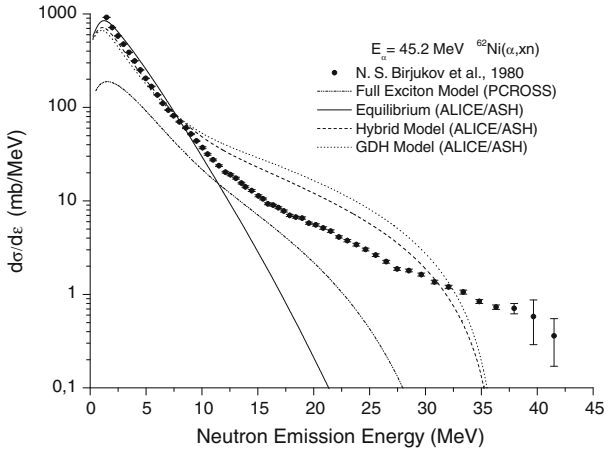


**Fig. 11** The comparison of neutron emission spectra of $^{62}$Ni(α,*xn*) reaction with the values reported in literature at 45.2 MeV incident neutron energy. Experimental values were taken from Ref. [53]

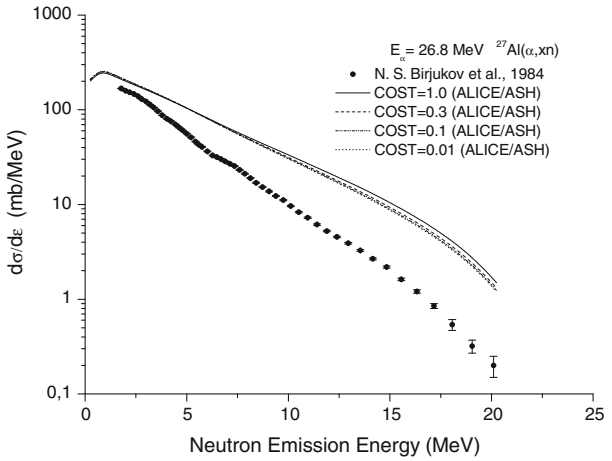


**Fig. 12** The comparison of some (COST) mean free path parameter values by using GDH Model (ALICE/ASH) for neutron emission spectra from the reactions $^{27}$Al(α,*xn*)

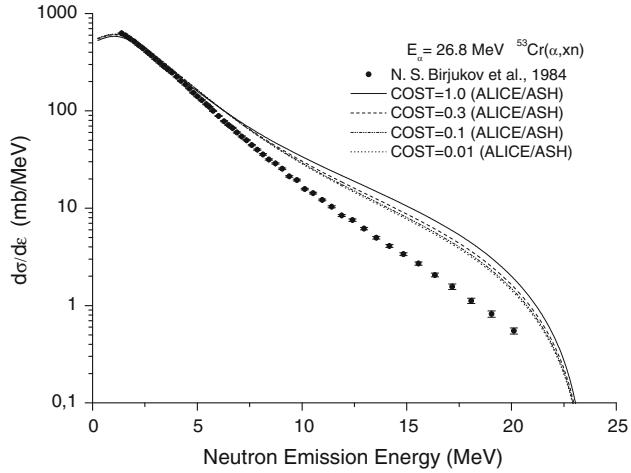


**Fig. 13** The comparison of some (COST) mean free path parameter values by using GDH Model (ALICE/ASH) for neutron emission spectra from the reactions $^{53}$Cr(α,*xn*)

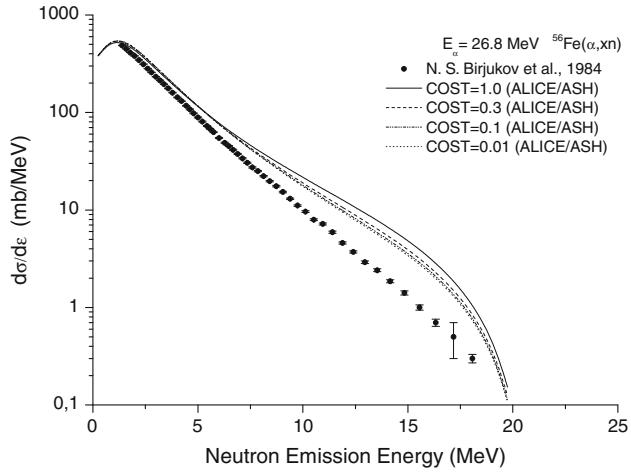


**Fig. 14** The comparison of some (COST) mean free path parameter values by using GDH Model (ALICE/ASH) for neutron emission spectra from the reactions $^{56}$Fe(α,*xn*)

the new developed pre-equilibrium reaction mechanism ALICE/ASH includes angular momentum conversion and so it gives us more information for new nuclear reaction researchers. When taking the pairing energy and the mass shell correction into consideration, the experimental values are in better agreement with the theoretical results.

The calculated results using the PCROSS code of the full exciton model have been given in Figs. 1, 2, 3, 4, 5, 6, 7, 8, 9, 10, and 11. The pre-equilibrium calculations have been investigated using the full exciton model for the neutron emission spectra produced from $^{27}$Al, $^{53}$Cr, $^{56}$Fe and $^{58,60,62}$Ni reactions for an incident energy 26.8 and 45.2 MeV. In general, the calculated results using the PCROSS code of the full exciton model are harmony with the experimental data emission energy ranges of 5–15 and 10–20 MeV. These calculations are lower than the

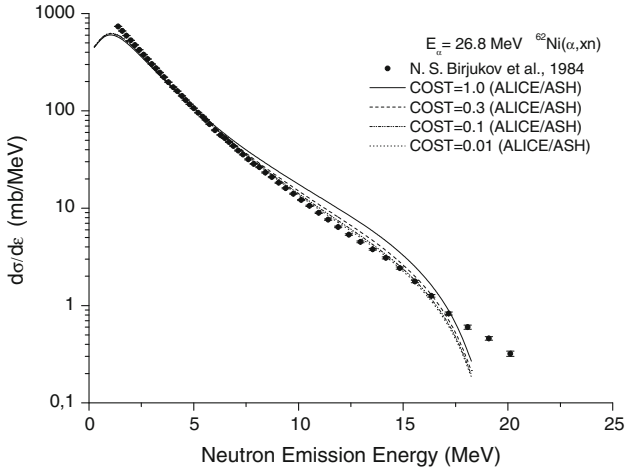


**Fig. 15** The comparison of some (COST) mean free path parameter values by using GDH Model (ALICE/ASH) for neutron emission spectra from the reactions $^{62}$Ni(α,*xn*)

experimental values at emission spectra energies of $E < 5$ MeV and $E > 20$ MeV.

The transition rate calculation involves the introduction of the parameter of mean free path determines the mean free path of the nucleon in the nuclear matter. The mean free path $k_{\mathrm{mfp}}$ parameter allows an increase in mean free path, with simulation of effects, which are not considered in the calculations, such as conservation of parity and angular momentum in intra nuclear transitions. The mean free path parameter, $k_{\mathrm{mfp}}$ in ALICE/ASH code is controlled by the COST value which is the multiplication factor for nucleon free path. We have investigated the multiple pre-equilibrium matrix element constant from internal transition for $^{27}$Al(α,*xn*), $^{53}$Cr(α,*xn*), $^{56}$Fe(α,*xn*) and $^{62}$Ni(α,*xn*) neutron emission spectra at 26.8 alpha incident energies for the GDH model calculations (Figs. 12, 13, 14, 15). For all reaction calculations, COST = 0.01 value corresponds to the experimental values in Figs. 12, 13, 14, and 15.

## References


1. Y. Wu, Plasma Sci. Technol. **3**(6), 1085 (2001)
2. Y. Chen, Y. Wu, Fusion Eng. Des. **49 & 50**, 507 (2000)
3. Y. Wu et al., Fusion Eng. Des. **51 & 52**, 395 (2000)
4. Y. Wu, in *International Symposium on Fusion Nuclear Technology*, San Diego, USA, 7–13 April 2002
5. S.J. Zinkle et al., J. Nucl. Mater. **258–263**, 205 (1998)
6. D.L. Smith et al., Fusion Eng. Des. **41**, 7 (1998)
7. H. Matsui et al., J. Nucl. Mater. **233–237**, 92 (1996)
8. W.R. Johnson, J.P. Smith, J. Nucl. Mater. **258–263**, 1425 (1998)
9. N.P. Taylor, C.B.A. Forty, J. Nucl. Mater. **283–287**, 28 (2000)
10. E.T. Cheng, J. Nucl. Mater. **258–263**, 1767 (1998)
11. Q. Huang et al., J. Nucl. Mater. **307–311**, 1031 (2002)
12. P.M. Raole et al., Trans. IIM **62**, 2–105 (2009)
13. M. Victoria et al., Nucl. Fusion **41**(8), 1047 (2001)
14. K. Ehrlich, Philos. Trans. R. Soc. Lond. A **357**, 595 (1999)
15. E.T. Cheng, J. Nucl. Sci. Technol. **2**, 1127 (2002)
16. D.R. Harries, Ferritic martensitic steels for use in near term and commercial fusion reactors. Paper presented at Top. Conf. on Ferritic Alloys for Use in Nuclear Energy Technologies, Snowbird, Utah, 1983
17. Y. Han et al., Nucl. Instrum. Methods Phys. Res. B **239**, 314 (2005)
18. N.L. Singh et al., Can. J. Phys. **76**, 10–785 (1998)
19. S.J. Iwata, J. Physical Soc. Japan **17**, 1323 (1962)
20. F. Tárkányi et al., Nucl. Instrum. Methods Phys. Res. B **207**, 381 (2003)
21. T. Nishio et al., J. Nucl. Sci. Technol. **2**, 955 (2002)
22. H.A. Yalım et al., J. Fusion Energ. **29**, 1–55 (2010)
23. E. Tel, Phys. Rev. C **75**, 034614 (2007)
24. M. Blann, Phys. Rev. Lett. **27**, 337 (1971)
25. M. Blann, Annu. Rev. Nucl. Sci. **25**, 123 (1975)
26. C.K. Cline, M. Blann, Nucl. Phys. A **172**, 225 (1971)
27. J.J. Griffin, Phys. Rev. Lett. **17**, 478 (1966)
28. G.D. Harp et al., Phys. Rev. **165**, 1166 (1968)
29. G.D. Harp, J.M. Miller, Phys. Rev. C **3**, 1847 (1971)
30. M. Ismail, Pramana **32**(5), 605 (1989)
31. J.S. Zhang, X.J. Yang, Z. Phys. A **329**(1), 69 (1988)
32. W. Dilg et al., Nucl. Phys. A **217**(2), 269 (1973)
33. F.C. Williams, Nucl. Phys. A **166**(2), 231 (1971)
34. D. Wilmore, P.E. Hodgson, Nucl. Phys. **55**, 673 (1964)
35. F.D. Becchetti, G.W. Greenlees, Phys. Rev. **182**, 4–1190 (1969)
36. J.R. Huizenga, G. Igo, Nucl. Phys. **29**, 462 (1962)
37. V.F. Weisskopf, D.H. Ewing, Phys. Rev. **57**, 472 (1940)
38. K.K. Gudima, S.G. Mashnik, V.D. Toneev, Nucl. Phys. A **401**, 329 (1983)
39. M. Blann, H.K. Vonach, Phys. Rev. C **28**, 1475 (1983)
40. H. Feshbach, A. Kerman, S. Koonin, Ann. Phys. (NY) **125**, 429 (1980)
41. T. Tamura, T. Udagawa, H. Lenske, Phys. Rev. C **26**, 379 (1982)
42. M. Blann, J. Bisplinghoff, CODE ALICE/LIVERMORE 82 UCID-19614 (1982)
43. M. Blann, A. Mignerey, W. Scobel, Nukleonika **21**, 335 (1976)
44. C.K. Cline, Nucl. Phys. A **210**, 590, 32 (1973)
45. C.K. Cline, Z. Phys. A **287**, 319 (1978)
46. M. Blann, A. Mignerey, Nucl. Phys. A **186**, 245 (1972)
47. H. Machner, Z. Phys. A **302**, 125 (1981)
48. C.H.M. Broeders, A.Y. Konobeyev, Y.A. Korovin, V.P. Lunev, M. Blann, ALICE/ASH—pre-compound and evaporation model code system for calculation of excitation functions, energy and angular distributions of emitted particles in nuclear reactions at intermediate energies, FZK 7183, May 2006, http://bibliothek.fzk.de/zb/berichte/FZKA7183.pdf
49. A.V. Ignatyuk, K.K. Istekov, G.N. Smirenkin, Yad. Fiz. **29**, 875 (1979) [Sov. J. Nucl. Phys. **29**, 450 (1979)]
50. M. Blann, Code ALICE-91, PSR-146, Statistical Model Code System with Fission Competition, Oak Ridge National Laboratory, RSICC Peripheral Shielding Routine Collection, Lawrence Livermore National Laboratory, Livermore, California and IAEA
51. R. Capote et al., Final Report on Research Contract 5472/RB, INDC(CUB)-004 (Higher Institute of Nuclear Science and Technology, Cuba), Translated by the IAEA on March 1991 (PCROSS program code)
52. E. Tel et al., Mod. Phys. Lett. A **19**(21), 1597 (2004)
53. Brookhaven National Laboratory, National Nuclear Data Center, EXFOR/CSISRS (Experimental Nuclear Reaction Data File). Database version of January 01, 2010, http://www.nndc.bnl.gov/exfor/